ISSN: 2664-9640

Simulation of carbide tool milling wear

Cheng Gong

Sichuan university of science and engineering, Yibin 644000, China

Abstract

In this paper, the thermodynamics and tool wear rate of stainless steel workpiece milling with carbide tool are analyzed. The tool wear rate was calculated by analyzing the three - direction force and temperature of the blade. The cutter - workpiece milling model was established, and the thermal change of cemented carbide cutter was analyzed by finite element analysis, so as to obtain the influence rule of different process parameters on cemented carbide cutter wear.

Keywords

Thermodynamics; Tool wear rate; Carbide cutter.

1. Introduction

Milling is a kind of mechanical processing, which can carry out rough milling, semi-finishing milling, finishing milling and other processing processes, its dimensional accuracy can reach the highest 0.01mm, surface roughness can reach 0.63~1.6μm. Stainless steel contains more Cr and Ni elements and changes the physical and chemical properties of the alloy, greatly enhancing its corrosion resistance, and still has high strength at higher temperatures (>450℃)[1]. However, due to the existence of stainless steel hardness, low thermal conductivity problems, in the process of milling force and heat, aggravate the tool wear [2-3]. Thus, frequent downtime is required to replace the tool, resulting in reduced milling efficiency. There are a lot of researches on tool wear in cutting process by many scholars at home and abroad. Xue Qinghua [4] studied the milling of 45 steel with carbide milling cutter, and found that the influence of cutting speed, cutting width, cutting depth and feed per tooth on tool life decreased significantly in turn, and established a numerical model of tool life and milling parameters. Sun Pengcheng [5] used single-factor test method to conduct experimental research on milling titanium alloy with carbide coated milling cutter, and explored the significance of the influence of various cutting parameters on the cutting force.

In this paper, the tool wear rate is calculated, and the influence of various process parameters on tool wear is studied when the carbide tool is milling stainless steel. Finally, the significant relationship between process parameters and tool wear is obtained.

2. Numerical model of tool wear

With the improvement of physical properties such as strength and hardness of materials, the metal cutting process becomes more difficult. In the contact area between the tool and the workpiece, the wear forms are diverse. Generally speaking, the main reasons for the normal wear of the tool are abrasive wear, bonding wear, diffusion wear, oxidation wear and so on[6].

2.1. Abrasive wear

According to their previous experience, g. Gei et al[7]. Divided the wear process of cemented carbide tools into the following steps: 1) the bonding phase movement of the alloy surface layer; 2) Plastic deformation of bonding phase; 3) The plastic strain of WC grain increases; 4) Fracture of single WC grains; 5) Intergrain fracture; 6) The grain is pulled out from the matrix.The

ISSN: 2664-9640

complex relationship between the back tool surface and the machined surface of workpiece makes the back tool surface wear. The volume of hard alloy material spalling on unit sliding distance can be expressed as:

$$Q_a = C_1 \cdot \mathrm{N}_{WC} \frac{\left(\frac{E}{H_V}\right) P^{\frac{9}{8}}}{K_C^{\frac{1}{2}} H_V^{\frac{5}{8}}} \tag{1}$$

Where C_1 is the constant independent of material, E is the elastic modulus of cemented carbide, HV is the Vickers hardness value of cemented carbide, KC is the fracture toughness, P is the load, and NWC is the number of micro-convex body per unit length on the tool surface.

When the cutting speed is V, within t time, the abrasive wear rate of the carbide tool's rear tool surface is:

$$\frac{Q_a}{\triangle t} = C_1 \cdot \mathrm{N}_{WC} \cdot v \frac{\left(\frac{E}{H_V}\right) P^{\frac{9}{8}}}{K_C^{\frac{1}{2}} H_V^{\frac{5}{8}}} \tag{2}$$

According to Nie Hongbo's research on measuring elastic modulus of cemented carbide by three-point bending method, the functional relationship between the content of Co in cemented carbide and elastic modulus E can be expressed as:

$$E = 0.13 f_{Co}^2 - 14.24 f_{Co} + 708.41 \tag{3}$$

According to the Vickers hardness of cemented carbide provided by H. Engqvist[8], it can be obtained:

$$H_V = \left(H_{WC} - H_{Co}\right) \cdot e^{\frac{-\lambda}{k}} + H_{Co} \tag{4}$$

According to Garland theory[9]:

$$\lambda = \frac{1 - f_{WC}}{N_{WC}} = \frac{f_{Co}}{N_{WC}} \tag{5}$$

In the above formula, K represents the parameters related to materials, d_{WC} represents the grain size of cemented WC, f_{Co} represents the volume fraction of bonded Co in cemented carbide, and λ is the mean phase free path of cobalt.

$$\frac{Q_a}{\triangle t} = C_1 \cdot P^{\frac{9}{8}} \cdot v \frac{\left(0.13 f_{Co}^2 - 14.24 f_{Co} + 708.41\right)}{\left(\left(a + \frac{b}{\sqrt{c + d_{WC}}} - 304 - \frac{12.7}{\sqrt{f_{Co} \cdot d_{WC}}}\right) e^{\frac{f_{Co} \cdot d_{WC}}{k}} + 304 + \frac{12.7}{\sqrt{f_{Co} \cdot d_{WC}}}\right)^{\frac{13}{8}}} \tag{6}$$

2.2. Adhesion wear

In the process of cutting, there is intense friction between the cutting tool surface and chip, and between the cutting surface and the machined surface. Because of the friction and the plastic deformation of chip, high temperature and high pressure physical phenomena are generated in the contact area. In this case, cold welding occurs in the contact area as a result of the adsorption between atoms on the new surface formed by the plastic deformation of the chips[10]. Due to the continuous cutting, the grain at the cold welding joint is torn under the conditions of alternating stress, contact fatigue and surface structural defects of the tool, and is taken away by the other side to form bond wear.

ISSN: 2664-9640

Archard J F has derived and established the calculation formula of tool adhesion wear rate[11]. It is assumed that the contact surface is composed of many similar micro-convexes, and the two micro-convexes touch each other and slip relative to each other. If the adhesion area of the two micro-convexes seems to be a circle with radius A, the formula of the contact area is as follows:

$$\delta A = \pi a^2 = \frac{\delta W}{\sigma_s} \tag{7}$$

Where, is the maximum load borne by a single micro-convex body; Is the material yield limit of the workpiece.

In the relative sliding process, the sliding distance of the surface on the micro-convex body is proportional to the area of the contact point. If assuming condition = 2a, then the sliding distance is, and the wear volume at is:

$$\frac{\delta Q_{ab}}{\delta L} = \frac{2\pi a^3}{3 \cdot 2a} = \frac{\pi a^2}{3} = \frac{1}{3}\frac{\delta W}{\sigma_s} \tag{8}$$

The total contact area corresponds to the total load. Considering that chips are generated in some (probability constant) parts of all contact microconvex bodies, the total wear volume at sliding distance L is:

$$Q_{ab} = \frac{1}{3}\frac{\delta W}{\sigma_s} \cdot K_{abl} \cdot L \tag{9}$$

The wear volume rate of the cutting tool during t time is:

$$\frac{\Delta Q_{ab}}{\Delta t} = \frac{1}{3}\frac{\delta W}{\sigma_s} \cdot K_{abl} \cdot V \tag{10}$$

In the process of tool wear, the wear depth, the average wear width and the length of the cutting edge change simultaneously[12]. It is assumed that the wear depth of the back tool surface and the wear amount of the cutting edge length are linear with the mean wear width of the back tool surface. There are:

$$Q \propto {V_B}^3 \tag{11}$$

The comprehensive results are as follows:

$$\frac{\Delta Q_{abl}}{\Delta t} = \frac{e_{ab} \cdot \left(\Delta V_B\right)^3}{\Delta t} = \frac{1}{3}\frac{\delta W}{\sigma_s} \cdot K_{abl} \cdot V \tag{12}$$

Where, is the scaling coefficient of wear volume and; Is the average temperature of the rear blade surface (K).

2.3. Diffusion wear

During cutting, the chemical elements of the chip, workpiece and tool are diffused from each other in the solid state during contact. The chemical elements that improve the tool hardness (such as W, Co, Ti, etc.) diffuse to the workpiece with a lower concentration of such elements, while the chemical elements in the workpiece material (Fe, C, etc.) diffuse to the tool, with the above two changes in the tool material becomes more brittle, and the workpiece hardness has a certain increase, thus accelerating the tool wear[13]. The diffusion rate of chemical elements on both sides is mainly related to the cutting temperature, and according to E-E /Ke. In exponential form [](e is the absolute temperature on the tool surface, E is the active chemical energy, K is a constant), meanwhile, the flow velocity of chip and tool surface, the chemical composition of tool and workpiece material have a certain influence on the diffusion velocity.

WC particles and 06Cr19Ni10 stainless steel, under high temperature and high pressure environment has a relatively stable chemical state. However, in the cutting process, the stability of cemented carbide binder is not as good as WC particles and 06Cr19Ni10 stainless steel.

ISSN: 2664-9640

Therefore, the diffusion of binder in milling process causes the loss of tool body. Therefore, within δ T time, the diffusion wear rate of hard tool rear face can be expressed as [14] :

$$\frac{Q_b}{\Delta t} = C_2 \cdot e^{-\frac{E}{R \cdot T}} \tag{13}$$

Where, C1 is the constant related to the microstructure of cemented carbide, E is the activation energy of diffusion, R is the gas constant, and T is the average temperature in the contact area between the tool surface and the processed surface.

3. Carbide tool milling simulation

The thermo-mechanical coupling simulation of milling stainless steel with carbide tool was carried out based on ABAQUS platform. BBD orthogonal test scheme (response surface analysis) was selected to study the influence of process parameters on tool wear when multiple factors change together. The relationship between process parameters and cutting force, milling temperature and tool wear is analyzed.

3.1. Design of test method

Orthogonal design method through orthogonal table and empirical formula to establish the test scheme, this method can design a representative test combination, using BBD orthogonal test for grouping, determine the level of each factor is 5, factor change spacing, avoid the shortage of the full factor test design more tests.

In data processing, the test to obtain the data filter and fitting, to extract the effective data analysis, data processing methods are polynomial fitting, average, data analysis methods mainly include multiple sets of test curve contrast analysis, variance analysis, the response surface analysis, through the reasonable design of experiment and data processing and analysis, Multiple sets of data and objective and correct conclusions can be obtained.Combined with engineering practice and reference to relevant literature, the value range of milling process parameters is determined as follows: The axial cutting depth is 0~10mm, Spindle speed is 1000~2000r/min, Feed per tooth is 0.3~0.5mm/z, The axial cutting depth is 0~5mm.

Table 1 Horizontal coding table of milling process parameters and factors

The level of	factors			
	Spindle speed	The radial cutting depth	The axial cutting depth	Feed per tooth
γ	1000	1	2	0.3
1	1250	2	4	0.35
0	1500	3	6	0.4
-1	1750	4	8	0.45
$-\gamma$	2000	5	10	0.5
Δ_j	250	1	2	0.05

ISSN: 2664-9640

3.2. Finite element simulation of carbide tool

In order to avoid grid distortion and difficult convergence in discrete simulation and ensure the accuracy of simulation, assembly modules are selected to create assemblies from components, and instance types are non-independent (grid components are divided separately). Because the blade part of the tool is a free-form surface and the structure is complex, the blade and the handle should be separated into separate grids. Tetrahedral meshing has strong adaptability, and the complex spiral surface of the blade part can be meshed quickly. The relative meshing technology is adopted in the meshing of the tool, and the initial total number of meshing of the tool and the workpiece is set to 80000 and 40000 respectively. The weight coefficient of the mesh window was adjusted to 1. The square window and the circular window were selected respectively to determine the mesh thinning position of the cutter-workpiece. The size ratio of inside and outside the window was 0.01.

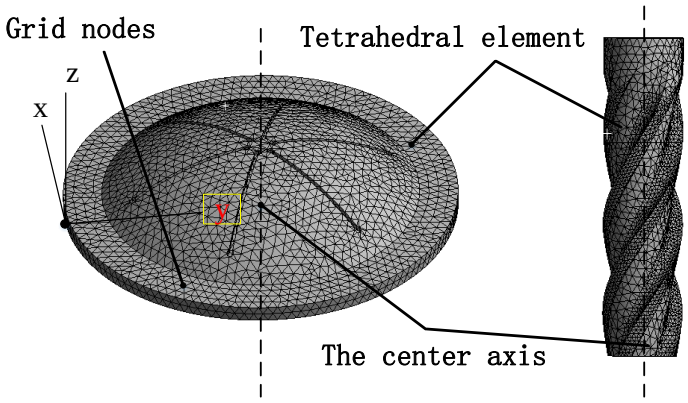

Figure 1 Cutter - workpiece 3d model mesh division

In order to obtain the milling force and milling heat between cutter and workpiece during milling, a local coordinate system was established with the cutter contact on the bursting disc as the origin, and the forward direction of the x axis was determined as the cutter feed direction, and the forward direction of the Z axis was determined as the normal vector of the cutter contact surface. The temperature boundary condition is added at 0 point, and the grid type is thermo - mechanical coupling to simulate the milling process of 06Cr19Ni10 stainless steel. The local coordinate system, load addition and boundary condition are added as follows.

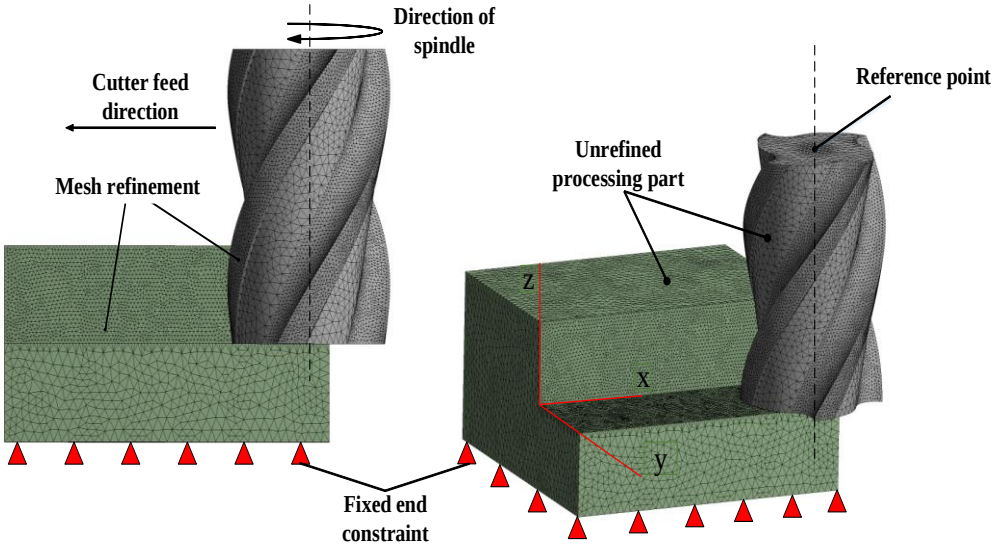

Figure 2 Local coordinate system, load application and boundary conditions

To complete the finite element milling simulation, it is necessary to set the milling simulation path, and the path is realized through multiple analysis steps. The analysis steps of the tool milling wear simulation model are set as 30 steps, and 30 steps are evenly distributed on the

ISSN: 2664-9640

tool milling path, so as to collect the load and heat data of the blade contact points. The analysis type adopts thermal-mechanical coupling and transient response, and the initial incremental step is set to 0.1. The field output takes the default option.

According to the numerical model of milling tool wear, ABAQUS was used to obtain the variation of three - way milling force and milling temperature during blade milling.

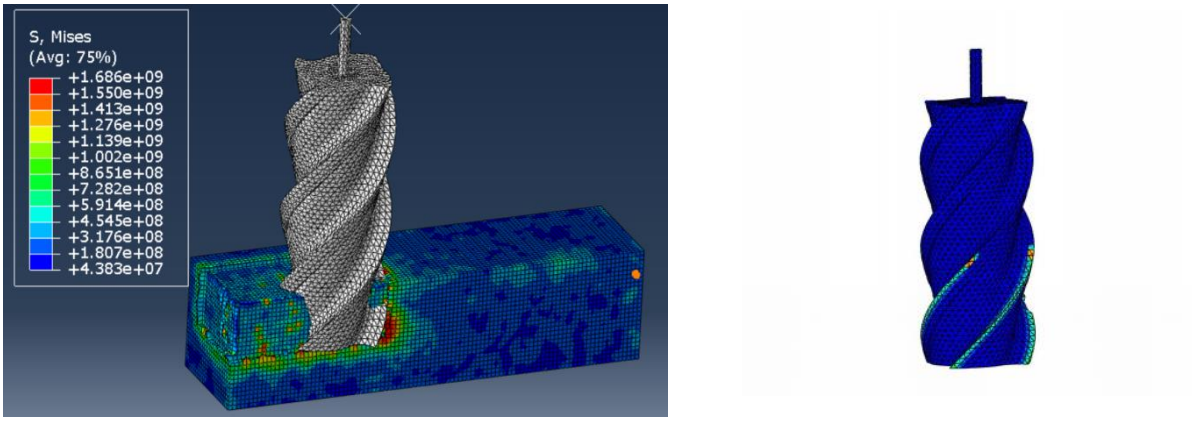

Figure 3 Milling stress and temperature

4. Three - way cutting force calculation

In the milling process, because the feed parameters used in milling are much smaller than the axial cutting depth, the four cutting edges of the milling cutter basically participate in the cutting at the same time. Therefore, intermittent effects between cutting edges can generally be ignored. In this way, the equivalent of orthogonal cutting in the form of cutting. The milling force of four - edge carbide milling cutter is analyzed[15].

According to the metal cutting theory, the sectional area of the cutting layer (A_D) is equal to the product of the radial cutting depth (A_C) and the cutting thickness (b_D), namely:

$$A_D = a_c \cdot b_D \tag{14}$$

$$a_C = f_z \cdot sin\theta \cdot sink_r \tag{15}$$

$$b_D = \frac{a_p}{\sin k_r} \tag{16}$$

Where :f_z=03~0.5mm, is the linear expansion coefficient of fluid, ap=1~10mm, k_r=90°, and the main deflection Angle. At the start of work, the external and tool temperature is 20 ℃. Therefore, Δt is the difference between the external environment and the actual operating temperature. Δt=0℃, θ instantaneous contact Angle, ψ is the maximum contact Angle.

When the radial cutting depth is constant, the cutting thickness varies with the instantaneous contact Angle, and the maximum cutting thickness is obtained when θ=ψ.

$$a_{cmax} = f_z \cdot sin\psi \tag{17}$$

$$\cos\psi = \frac{\frac{D_c}{2} - a_e}{\frac{D_c}{2}} = 1 - \sqrt{1 - \cos^2\psi} \tag{18}$$

Combining formula 17 and 18, it can be obtained:

$$a_{cmax} = f_z \cdot \sqrt{1 - cos^2\psi} \tag{19}$$

When the radial cutting depth is close to the cutting radius, the feed per tooth can be approximated as the maximum cutting width.

ISSN: 2664-9640

$$A_{Dmax} = a_c \cdot b_D \approx f_z \cdot a_p \tag{20}$$

$$F = \frac{\tau \cdot A_D}{\sin\phi \cdot \cos\phi\left(\phi - \beta - \gamma_0\right)} \tag{21}$$

Among:τ is the shear stress on the shear surface, and β is the friction Angle between the front cutter surface and the chip. φ is the shear Angle, γ_0 is the carbide tool Angle, λ is the main cutting edge Angle.

According to the dynamic mechanical properties of materials, shear stress is closely related to strain, strain rate and temperature.

$$\tau = f(\varepsilon, \dot{\varepsilon}, T) \tag{22}$$

Among:ε is strain, $\dot{\varepsilon}$ is strain rate,T shear surface temperature.

In the normal plane of the cutting edge, the cutting force F_r along the tool feed direction can be obtained, and the function of the cutting force F_n perpendicular to the workpiece surface can be written:

$$F_n = Fsin(\beta - \gamma_0) \qquad F_r = Fcos(\beta - \gamma_0) \tag{23}$$

The force in cutter section is transformed into cartesian coordinate system and the three - direction milling force component is obtained.

$$\begin{cases} F_x = F_n \cos\psi + F_r \cos\lambda \sin\psi \\ F_y = F_n \sin\psi + F_r \cos\lambda \cos\psi \\ F_z = F_r \sin\lambda \end{cases} \tag{24}$$

From the above three equations, it can be seen that in the cutting process of a milling cutter tooth, the cutting force perpendicular to the feed direction and parallel to the feed direction changes with the change of the instantaneous position Angle of the cutter tooth, and the axial force is only related to the edge Angle and the front Angle of the end edge.

5. Analysis of Simulation Data of Cemented Carbide Tool Milling

According to the designed test plan, the milling parameter combination of each group is different. Pro-E software is used to establish a three-dimensional milling model according to each parameter combination, and the milling simulation of the model is completed in ABAUQUS, and the three-way milling force and milling temperature data are output. After the calculation is completed, observe the tool wear rate in the post-processing interface, and import the obtained wear rate data into Origin for data processing to obtain usable data. Extract three-way milling force, milling temperature and tool wear rate data The simulation test result data is as follows .

Table 2 BBD orthogonal test simulation results

Serial number	F_x	F_y	F_z	T/℃	Tool wear rate
1	724.75	712.25	89.51	342.28	0.00525
2	814.26	796.57	105.42	334.72	0.00634
3	742.79	718.65	102.94	392.43	0.00497
4	809.36	793.08	98.81	352.34	0.00591
5	823.68	814.05	110.89	376.58	0.00648
6	847.65	831.84	108.94	358.64	0.00664

ISSN: 2664-9640

7	815.06	792.49	92.67	362.73	0.00613
8	825.66	809.34	87.56	368.73	0.00543
9	844.73	824.98	96.32	340.59	0.00571
10	826.42	797.88	94.71	402.13	0.00542
11	883.55	842.59	166.32	466.72	0.00732
12	804.68	781.39	89.12	384.37	0.00464
13	846.57	814.36	118.99	441.31	0.00588
14	821.53	784.32	86.63	413.68	0.00493
15	823.83	799.34	94.87	403.62	0.00481

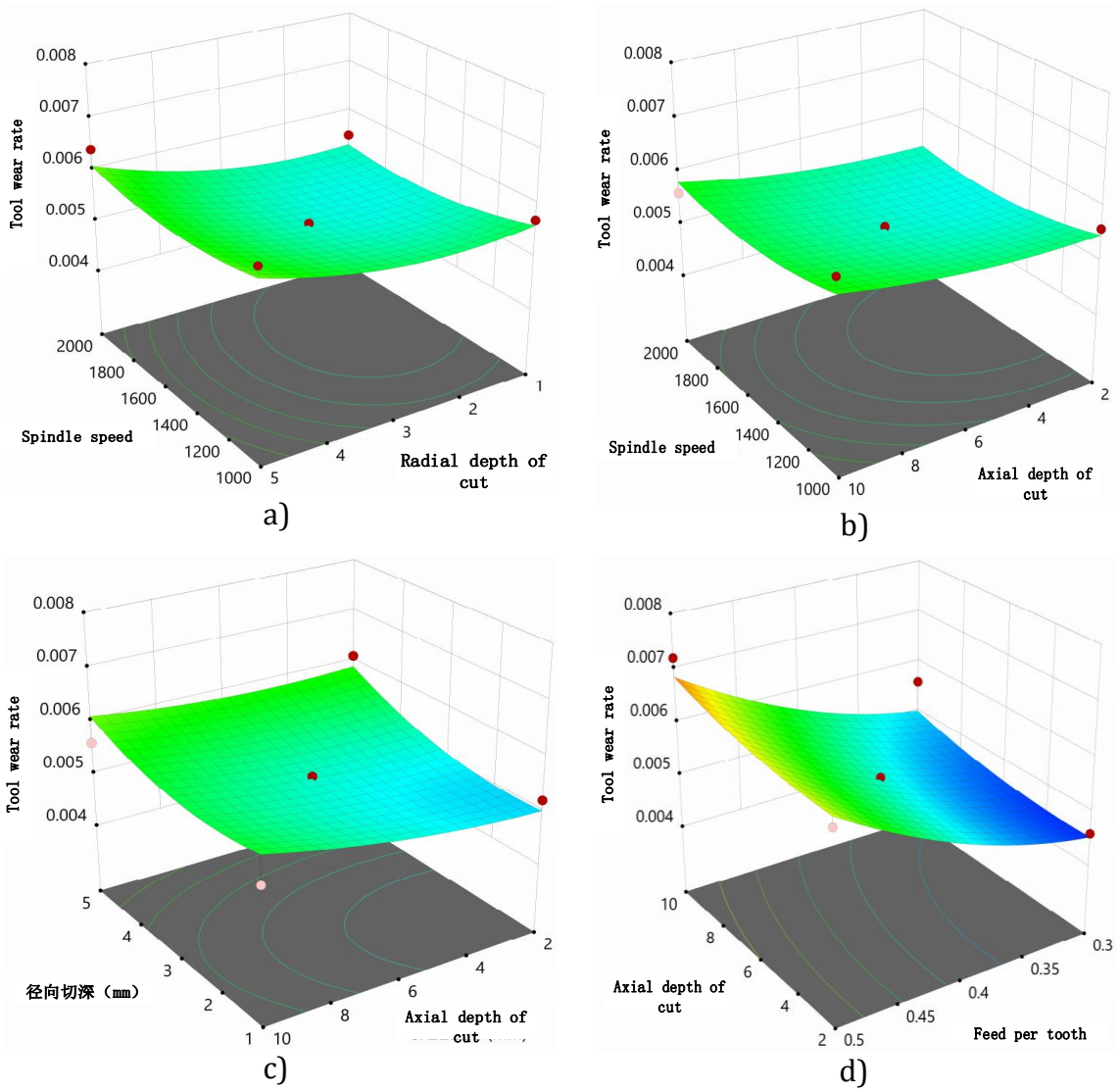

Figure 4 Response surface

The test data adopts Design-Expert software to analyze and study the influence degree of each machining process parameter on the tool wear rate.

According to the characteristics of the model and the relationship between the design variables and the response, the design-Expert software extracts the input 4 factors and the output

ISSN: 2664-9640

response surface of the tool wear rate. When drawing the relationship between the two factors and the response, the other two factors Keep the zero level unchanged, the response between each factor and the tool wear rate is shown in the figure.

a) The tool wear rate, spindle speed and radial depth of cut show a "concave" law, that is, as the spindle speed increases, the wear rate shows a decreasing trend, but the overall degree of change is gentle, and the radial depth of cut The change makes the deformation change more drastically.

b) The tool wear rate increases with the increase of the axial depth of cut, and the spindle speed relative to the axial depth of cut makes the change of the tool wear rate weaker. When these two factors change together, the impact on the tool wear rate is not severe.

c) There is a "sag" phenomenon between the tool wear rate and the radial depth of cut. When the radial depth of cut and the axial depth of cut change together, the tool wear rate is affected severely. The wear rate when the axial depth of cut exceeds 6mm The changes are greater.

d) The tool wear rate increases with the increase of the feed per tooth and the axial depth of cut. The feed per tooth has a greater impact on the tool wear rate than the axial depth of cut.

Based on the above, there is a response graph showing the feed per tooth, and the tool wear rate changes drastically, but there is no response graph with the feed per tooth, and the change in the tool wear rate is relatively slow. Compared with the case where the two factors change together, as long as the change in the feed per tooth exists, the tool wear rate will change drastically. Therefore, it is concluded that when changing the process parameters under certain circumstances, the feed per tooth should be set as small as possible. Give the amount.

6. Conclusion

After the finite element simulation of all the BBD orthogonal test program groups, the maximum values of Fx, Fy, Fz and milling temperature of carbide tools can reach 883N, 842N, 166N and 466°C respectively; the minimum value of tool wear rate is 0.00464mm/h, the maximum is 0.00734mm/h. According to the calculation formula of cutting force, it is proved that the data of Fx, Fy, Fz are reasonable.

Through data analysis of thermo-mechanical coupling milling simulation, the influence law of each process parameter on the wear rate of cemented carbide tools is obtained. Spindle speed: With the increase of spindle speed, Fx and Fy show undulating changes, but the overall change trend of Fy and Fx is decreasing. Feed per tooth: With the increase of feed per tooth, Fx, Fy, Fz and milling temperature all show an upward trend. The three-way milling force rises gently, while the temperature rises more, indicating the feed per tooth The larger the value, the greater the milling force and heat generated during the milling process. The analysis reason is: as fz increases, it means that the milling thickness of each tooth increases, and the milling area increases, that is, the volume of material that needs to be cut out under the same standard is more , The greater the milling force and heat generated, the greater the corresponding increase. Axial depth of cut: As the axial depth of cut increases, Fx, Fy, and Fz all show an upward trend. This is because the axial depth of cut increases, the milling area increases, and the material removal rate becomes larger. Radial depth of cut: the three-directional milling force and milling temperature have a small increase in the range of 1 to 3mm in the radial depth of cut. After 3mm, the milling temperature will increase significantly, while Fx and Fy increase approximately linearly.

References

[1] Yin Fubin. Analysis of Milling Process of Austenitic Stainless Steel[J]. Science & Technology Innovation Herald, 2017, 14(10): 109-109.

ISSN: 2664-9640

[2] Dai Dengzhao, Zhou Houming, congratulations, Deng Jianxin. Experimental study on cutting force of ceramic tools in cutting austenitic stainless steel[J]. Machine Design and Manufacturing, 2011, (12): 252-254.

[3] Gao Yanling. Research on the processing characteristics of stainless steel materials[J]. Equipment Machinery, 2014(04): 62-65.

[4] Xue Qinghua. Research on tool life reliability of milling hardened 45 steel and 40Cr steel [D]. Jinan: Shandong University, 2013.

[5] Sun Pengcheng, Xu Xiaolei, Zhang Zheng, Li Junqi, Wang Zhibin, Su Jun, Zhang Bo, He Linlin, Wang Conghui, Hui Jun. Research on the influence of titanium alloy TC4 high-speed milling parameters on milling force[J]. Machine Tool and Hydraulics, 2020, 48 (14): 37-40.

[6] Lu Jiahe. Research on Tool Wear and Tool Geometrical Parameter Optimization for Cemented Carbide Plunge Milling[D]. Harbin University of Science and Technology, 2019.

[7] Nemetz A W,Daves W,Klünsner T,et al. FE temperature-and residual stress prediction in milling inserts and correlation with experimentally observed damage mechanisms[J].Journal of Materials Processing Technology,2018,256: 98-108.

[8] H. Engqvist, S. Jacobson, N. Axen. A model for the hardness of cemented carbides [J]. Wear, 2002(252): 384-393.

[9] Gee M G, Gant A, Roebuck B. Wear mechanisms in abrasion and erosion of WC/Co and related hardmetals [J]. Wear, 2007, 263(1): 137-148.

[10] Nie Hongbo. Three-point bending method to test the elastic modulus of cemented carbide field. Powder metallurgy materials science and engineering. 2010, 15(6): 606-610.

[11] Chen Xiaorun, Fang Yi, Tian Meili, et al. High-speed milling 1Cr18Ni9 stainless steel cutting force modeling and experimental analysis[J]. Tool Technology, 2007, 41(11): 33-35.

[12] Li Chao. Research on remaining life prediction of mechanical equipment based on monitoring data[D]. Dalian University of Technology, 2014.

[13] Marksberry P W, Jawahir I S. A comprehensive tool-wear/tool-life performance model in the evaluation of NDM (near dry machining) for sustainable manufacturing [J]. International Journal of Machine Tools & Manufacture, 2008,48(7): 878-886.

[14] Wang Xiaoqin. Research on Friction and Wear Characteristics and Tool Life of Qin Alloy Ti6A14V High-efficiency Cutting Tools [D]. Shandong University, 2009.

[15] Luigino Filice, Fabrizio Micari, Luca Settineri, et al. Wear modelling in mild steel orthogonal cutting when using uncoated carbide tools [J]. Wear, 2007(262):545--554.